Effects of Structural Disparities in Polymer Blends: A Monte-Carlo Investigation

M. Müller

Institut für Physik, Johannes Gutenberg Universität, Staudinger Weg 7, D-55099 Mainz, Germany

Received November 1, 1994; Revised Manuscript Received May 23, 1995[⊗]

ABSTRACT: In the present Monte-Carlo simulation, we study the effects of structural differences on the thermodynamic behavior of polymer blends within the framework of the bond fluctuation model. Two types of structural differences are investigated: nonadditivity induced by indented monomer shapes and different stiffnesses of the two components. In both cases we find evidence for a positive, chain length independent entropic contribution to the χ parameter. Within the semi-grand-canonical ensemble this contribution can be detected via corrections to the Flory–Huggins equation of state (SG-EQS) or a shift in the critical temperature. For mixtures with nonadditive monomers, we find an UCSP for repulsion between unlike species and short chain lengths and a LCSP for longer chains and attractive interactions. The simulation data are compared to a mean field approximation. The results of blends with different stiffnesses is in qualitative agreement with recent field theoretical calculations of Liu and Fredrickson.

1. Introduction

Polymer melts and blends have been the subject of intense scientific research over many years because there is large practical interest in "alloying" polymers of different chemical natures.[1–3] Since the properties of a mixture are not the linear superposition of the constituents' characteristics, blending may potentially result in new materials with exciting features. The deviation from the linear superposition is described by excess properties. Within the Flory–Huggins theory[4] of polymer blends the excess entropy of mixing is given exclusively by the combinatorial entropy, which is reduced by a factor $1/N$, compared to mixtures of small molecules. For polymer mixtures with identical monomer structures of both species this prediction is rather well obeyed far away from criticality. However, this property is supposed to rely crucially on the structural equivalence of the monomeric units. Since the degree of polymerization N is very large, polymers of different chemical natures are generally very incompatible. Due to this low combinatorical entropy gain upon mixing in polymers, other contributions to the excess entropy may become relevant in the long chain length limit. These additional entropic terms may arise from packing effects, which are induced by structural differences of the monomers. The relevance of structural asymmetries has been emphasized by both experiments[5,6] and theory.[7–9]

To illustrate the origin of entropic contributions, let us start from a mixture of two species of polymers denoted as A and B. For simplicity we restrict ourselves to the special case of equal degrees of polymerization $N_A = N_B \equiv N$. The canonical partition function $\mathcal{Z}$ of a mixture comprising n_A A polymers and n_B B polymers in a volume V is given by

$$\mathcal{Z}(n_A,n_B) = \frac{1}{2^{n_A+n_B} n_A! n_B!} \sum_{\{c\}} \exp(-\beta E(\{c\})) \quad (1.1)$$

where the prefactor takes account of the indistinguishability of chains of the same species and the head–tail symmetry. E represents the energy of inter- and intramolecular potentials and β is the inverse temperature. We define formally the partition function $\mathcal{Z}_A(\varrho,\beta)$ of an A chain in a mixture according to

$$\begin{aligned}\mathcal{Z}_A(\varrho,\beta) &= \frac{\sum_{\{n_A+1,n_B-1\}} \exp(-\beta E)}{\sum_{\{n_A,n_B-1\}} \exp(-\beta E)} \\ &= \langle \sum_{\{A\}} \exp(-\beta \delta E(\{A\})) \rangle_{\varrho,\beta} \\ &\equiv V(\exp(s_A(\varrho,\beta) - \beta e_A(\varrho,\beta)))^N \end{aligned} \quad (1.2)$$

where $\delta E(\{A\})$ denotes the energy change associated with the insertion of the $(n_A + 1)$th A polymer and $\varrho = n_A/(n_A + n_B)$ denotes the composition of the mixture. e_A and s_A describe the energy and entropy of an A monomer in the mixture of composition ϱ and temperature $1/\beta$. The normalization takes account of the fact that the free energy of a single chain is proportional to the chain length N. Therefore the quantities e_A and s_A are independent of N to leading order. With the corresponding definitions of e_B and s_B a relation between the composition ϱ and the exchange chemical potential $\Delta\mu \equiv \mu_A - \mu_B$ can be established in the following form:

$$\begin{aligned}\beta\Delta\mu &= \frac{1}{N} \ln \frac{\mathcal{Z}(n_A,n_B)}{\mathcal{Z}(n_A+1,n_B-1)} \\ &= \frac{1}{N} \ln \frac{\varrho}{1-\varrho} + \Delta S - \beta \Delta E \quad \text{(SG–EQS)} \end{aligned} \quad (1.3)$$

with

$$\Delta S = s_B - s_A \quad \text{and} \quad \Delta E = e_B - e_A$$

Within the mean field approximation for composition fluctuations,[4] the energy difference $\beta\Delta E$ related to transforming an A chain to a B chain can be replaced by the well-known Flory–Huggins term $\chi_0(2\varrho - 1)$. Here χ_0 denotes the bare, enthalpic monomer interaction. ΔS is related to the different number of chain conformations of A and B chains in a mixture.

[⊗] Abstract published in *Advance ACS Abstracts,* August 1, 1995.

0024-9297/95/2228-6556$09.00/0

In analogy to scattering experiments,[5,10] the derivative of the semi-grand-canonical equation of state (SG-EQS) or the Flory–Huggins equation of state (1.4) with respect to the composition defines an effective χ parameter:

$$\frac{1}{S_{\text{coll}}(\vec{k} \to 0)} \propto \frac{1}{L^3 \Phi_1 (\langle \varrho^2 \rangle - \langle \varrho \rangle^2)}$$
$$= \frac{1}{N\varrho} - \frac{1}{N(1-\varrho)} - 2\left(\chi_0 - \frac{1}{2}\frac{\partial \Delta S}{\partial \varrho}\right)$$
$$\equiv \frac{1}{N\varrho} - \frac{1}{N(1-\varrho)} - 2\chi_{\text{eff}} \qquad (1.4)$$

The segmental quantity χ_{eff} comprises an enthalpic contribution proportional to $1/T$ and a temperature independent entropic term. Such a behavior is also observed in many scattering experiments. The latter is related to the composition dependence of the chain conformations. As noted above, the entropic contribution is independent of chain length to leading order. Thus it may dominate the excess entropy of mixing in the long chain length limit.

Monte-Carlo simulations within the semi-grand-canonical ensemble are well suited to reveal the consequences of structural differences. In this ensemble the total number of monomers and the chemical potential difference $\Delta\mu$ or exchange potential is constant, while the composition ϱ is allowed to fluctuate. The semi-grand-canonical equation of state (SG-EQS) (1.4) relates the mean composition to the exchange potential. The Monte-Carlo moves which relax the composition, consist in switching the chain identity A $\rightleftharpoons$ B without modifying their spatial conformation and taking account of the associated energy change via the Metropolis criterion. Apart from these semi-grand-canonical moves, we employ local random hopping and slithering snake moves to relax the polymer conformations without changing the composition of the mixture. Since the effort is focused on the relaxation of the composition, the relaxation times and the critical slowing down in the vicinity of criticality is smaller than in the canonical ensemble. In combination with sophisticated finite size methods[11,12] and histogram reweighting methods,[13,14] computer simulations in the semi-grand-canonical ensemble have proven to be an efficient tool to investigate the thermodynamic behavior of symmetric polymer mixtures.[15,16] This scheme has been applied successfully to monomers with different "adhesive" energies[17] and generalized to mixtures of different chain lengths.[18,19] In the present paper, we want to exploit the rich structure of the bond fluctuation model[20] to mimic entropic contributions to the effective χ parameter by Monte-Carlo simulations of two model systems: blends of polymers with nonadditive monomer shapes and polymeric mixtures of different stiffnesses. The resulting deviations from the ideal Flory–Huggins behavior can be detected by a shift in the critical temperature or via additional contributions in the semi-grand-canonical equation of state. Since the latter is directly accessible in the semi-grand-canonical ensemble, Monte-Carlo simulations can provide information on thermodynamic properties even far away from the critical point. This is particularly important, because the analytical mean field like treatments of polymer blends often neglect composition fluctuations which may lead to rather large discrepancies between the mean field treatment and the actual behavior in the vicinity of the critical point.[16] In contrast to many experiments, different types of entropic effects can be isolated and studied separately. Thus the analysis is not complicated by the presence of qualitatively different disparities. Macroscopic thermodynamical properties as well as local, structural quantities are simultaneously accessible.

The outline of the remainder is as follows: In the next section we introduce a modification of the bond fluctuation model and discuss the consequences of indented monomer shapes within the framework of a mean field approximation. Then we present our simulational results, concerning the SG-EQS and the chain length dependence of the critical temperature. In the second part, we discuss the consequences of different chain stiffnesses on the thermodynamic behavior of blends by revealing a small entropic contribution to the athermal SG-EQS and a shift of the critical temperature. The results are compared to the prediction of the P-RISM theory of Schweizer[8] and field theoretical calculations of Liu, Fredrickson, and co-workers.[9] In a final section we present our conclusions and an outlook on future work.

2. Polymer Blends with Nonadditive Monomer Shapes

In the original lattice model used by Flory and Huggins[4] each segment is represented by a single site on a completely filled, simple cubic lattice. Due to the structural equivalence of A and B monomers and the lack of vacancies no packing effects occur. Therefore this simple lattice representation of a polymer mixture does not capture the influence of structural disparities on the thermodynamic behavior.

In the present investigation we use the bond fluctuation model, introduced by Carmesin and Kremer.[20] This coarse-grained lattice model of polymeric materials has been proven especially useful in studying universal features of polymer thermodynamics by computer simulation. A statistical segment, comprising a small number of chemical repeat units, is mapped onto a lattice monomer, such that the relevant features of polymeric materials are retained: connectivity of the monomers along a polymer and the excluded volume of the statistical segment. Each monomer occupies a whole unit cell of a simple cubic lattice. All lengths are measured in units of lattice constants, and periodic boundary conditions are applied throughout. The presence of vacancies permits local fluctuations of the density and gives rise to pronounced packing effects on the length scale of a few lattice constants.[19,21] Thus the bond fluctuation model combines the computational tractability of lattice models with some features of continuous space models. The N monomers along a polymer are connected via one of 108 bond vectors of the set P(2,0,0), P(2,1,0), P(2,1,1), P(2,2,1), P(3,0,0), and P(3,1,0), where P denotes all permutations and sign combinations. Working at a filling fraction $8\Phi = 0.5$ or 0.35 of occupied lattice sites, the model reproduces many characteristic features of a dense melt or concentrated solution, respectively. The chains obey Gaussian statistics $R^2 = c_N\langle b^2\rangle(N-1)$, where b denotes the bond length and $c_N \approx 1.4$ in the case of no bond angle potential. The screening length ξ of the excluded volume interactions is about 6.5 or 7.9 for $8\Phi = 0.5$ or 0.35.[22] When specific polymeric materials are mapped on a lattice model,[23] the monomeric interactions are transformed into effective interactions of the coarse-grained monomers. As in previous studies, the thermal interactions are modeled by a square well potential comprising all 54 neighbor sites up to a distance $\sqrt{6}$.[16] The contact of monomers of the same

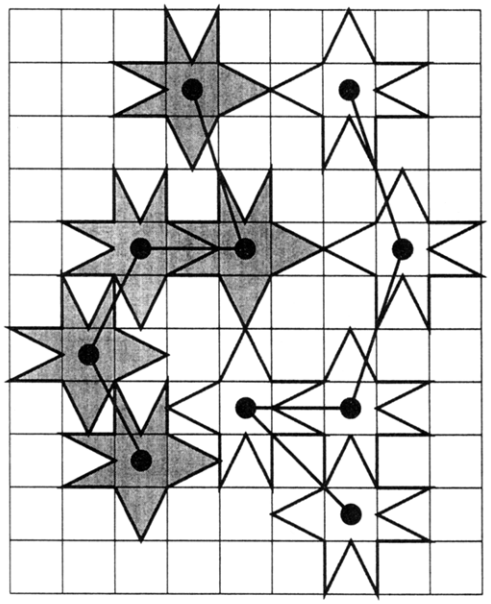

Figure 1. Illustration of the intended monomer structure. A monomers are shaded; B monomers, unfilled. The effect of the indentation can be described by a nonadditive hard core repulsion between monomers. As alluded, there is a strong entropic packing advantage which leads to phase separation.

species lowers the energy by ϵ, whereas the contact of different kinds increases the energy by the same amount.

In the present study, however, we also try to include packing effects induced via different monomer shapes or steric hindrances by describing the monomers of our coarse-grained lattice model as indented cubes. This is illustrated in Figure 1 for a two-dimensional analogon. As one can observe, monomers of different species must have a spatial distance greater than $\sqrt{5}$, whereas monomers of the same type may approach each other up to 2 lattice constants. Thus the net effect of these indentations is a nonadditivity between monomers of different species excluding the P(2,0,0) distance from occupancy. Of course, this extremely simple monomer shape is not a faithful representation of realistic monomeric packing structures on a microscopic length scale, but it is supposed to capture some universal, long wavelength features on the coarse-grained scale of Kuhnian segments. Note that the importance of the monomer shape and packing effects has been emphasized by the lattice cluster calculations of Freed and coworkers[7] and is used to explain the temperature dependence of the χ parameters in experimental studies.[10] Furthermore, a model with nonadditive hard cores and specific attractions between unlike species has been employed recently by Honeycutt[2] to investigate tacticity effects in PVC/PMMA blends. These calculations employ the P-RSIM theory with the atomic MSA closure. At large nonadditivity, Honeycutt finds a lower critical solution point (LCSP) whereas for small nonadditivity the blend is miscible at all temperatures. However, due to the known deficiencies of this atomic closure,[16] the author does not investigate the chain length dependence of the critical temperature.

Another practical advantage of the model above is the symmetry with respect to an exchange of the labels A and B. Therefore the coexistence value of the exchange potential $\beta\Delta\mu$ vanishes, and the phase diagram is symmetric about $\varrho = 1/2$. This renders the Monte-Carlo simulations in the semi-grand-canonical model much less demanding than for asymmetric models. For the pure phases $\varrho = 0, 1$ the model is equivalent to the original model and the nonadditivity has no effect at all. However it is obviously much easier to insert an A polymer into an A rich phase than into a B-rich one. Therefore the single chain entropy Ns_A of an A polymer increases strongly with the composition ϱ, whereas the opposite holds true for a B chain. According to the definition (1.4) this corresponds to a large positive contribution to χ_{eff}.

2.1. Mean Field Approximation. It is well-known that nonadditivity in mixtures of small molecules leads to an entropy-driven phase separation, because polymers in the pure phases pack more efficiently than a mixture.[24] For polymers this effect is supposed to be much more pronounced because of the low combinatorial entropy gain upon mixing. To quantify this effect, we resort to a simple mean field approximation. Consider the ratio of the canonical partition functions of an additive mixture $\mathcal{Z}_{add}$ and a blend with nonadditive monomer shape $\mathcal{Z}_{nadd}$:

$$\ln \frac{\mathcal{Z}_{nadd}}{\mathcal{Z}_{add}} = \ln \frac{\sum \exp(-\beta E)\Pi_{i,j}(1 - \delta(r_{ij} - 2))}{\sum \exp(-\beta E)} = \ln \langle \Pi_{i,j}(1 - \delta(r_{ij} - 2)) \rangle_{|add} \quad (2.5)$$

where the sum comprises all configurations of the additive mixture. The index i (j) runs through all monomers of type A (B) and the factor $(1 - \delta(r_{ij} - 2))$ excludes all configurations violating the nonadditivity constraint. Neglecting correlations among the monomer positions, one can factorize the average and gets to a first approximation:

$$\ln \frac{\mathcal{Z}_{nadd}}{\mathcal{Z}_{add}} \approx \sum_{i,j} \ln \langle (1 - \delta(r_{ij} - 2)) \rangle_{|add} \approx -\sum_{i,j} \langle \delta(r_{ij} - 2) \rangle_{|add} = -n_A n_B \frac{z_6}{V\Phi_{|}} = -V\Phi_{|}\varrho(1 - \varrho)z_6 \quad (2.6)$$

where z_6 corresponds to the mean number of particles at a distance 2 in an additive mixture and $\Phi_{|}$ denotes the monomer number density. This quantity is accessible in the simulation via the intermolecular pair correlation function in an additive mixture:

$$z_6 = \Phi_{|} \sum_{i=1}^{6} g_{AB}(\vec{x}_i)|_{add} \quad (2.7)$$

where the pair correlation function is normalized such that $g(r) \to 1$ for $r \to \infty$. Neglecting all local packing effects, one gets $z_6 = 0.2625$. Finally, the packing-induced contribution to the free energy and the effective χ parameter takes the form:

$$\frac{1}{\Phi_{|}}\beta\Delta f \approx z_6\varrho(1 - \varrho) \qquad \chi_{eff} = \chi_0 + z_6 = \frac{2z_c}{T} + z_6 \quad (2.8)$$

where z_c is the effective coordination number of the thermal interaction, i.e. the mean number of monomers of *other* chains within the range of the square well potential.[19] As anticipated, the effective χ parameter contains an enthalpic part and an entropic contribution. The excess entropy of mixing comprises two concurrent terms. The combinatorial entropy stabilized the mix-

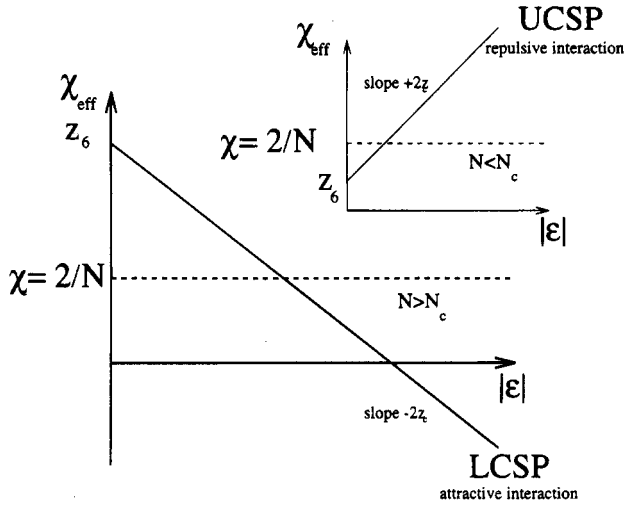

Figure 2. Qualitative behavior of the χ parameter for short chains (UCSP) and long (LCSP).

Table 1. Critical Temperatures for Mixtures of Nonadditive Monomers at a Density $8\Phi = 0.35$

N	ϵ_c	system size	
10	+0.01204(40)	28,40,50	UCSP
16	−0.0172(2)	46,56,64	LCSP
20	−0.0275(4)	40,57,80	LCSP
40	−0.0490(6)	40,55,80	LCSP

ture whereas the packing contribution favors phase separation. Since the former is reduced by a factor $1/N$, the packing entropy dominates the behavior in the long chain limit.

Therefore the mean field treatment gives the following qualitative predictions for the phase behavior (cf. Figure 2). The Gibbs criterion determines the critical temperature to

$$\chi_c = \frac{2}{N} = z_6 + 2\epsilon_c z_c \quad \Rightarrow \quad \epsilon_c = -\frac{z_6}{2z_c}\left(1 - \frac{2}{z_6 N}\right) \tag{2.9}$$

Thus there exists a critical chain length $N_c = 2/z_6$. In the absence of thermal interactions there is no temperature scale, and the athermal system is miscible for $N < N_c$ or immiscible in the case of $N > N_c$, respectively.[25] To observe a thermally driven phase transition for $N < N_c$, one has to introduce a repulsive interaction between different species, $\epsilon > 0$, leading to an upper critical solution point. The qualitative behavior for short chain lengths remains therefore unchanged. For $N > N_c$, however, the athermal system is immiscible. Therefore one has to introduce an attraction, $\epsilon < 0$, between different species to observe a thermally driven transition. Below the critical temperature the energetical attraction dominates and the system becomes misicble; i.e. one finds a lower critical solution point. With growing chain length the lower critical solution temperature approaches a finite value from above. Despite the crudeness of this simple factorization approach, it serves as a guideline for the analysis of the simulation data.

2.2. Simulational Results: Semi-Grand-Canonical Equation of State, χ Parameter, and Critical Temperature. In contrast to earlier investigations,[16,19] we work at a monomer number density $8\Phi = 0.35$. For the pure phase this represents a concentrated solution,[22,26] whereas for mixed composition the effective density is somewhat higher due to the additional excluded volume of the nonadditivity. For each semi-grand-canonical switch, six neighboring lattice sites per monomer must not be occupied by monomer centers of other chains of the same species. Therefore the acceptance rate for this type of Monte Carlo moves decreases rapidly with growing chain length. However up to chain length $N \leq 40$ the slightly reduced total monomer density compared to earlier studies[16] guarantees sufficient small relaxation times of composition fluctuations.

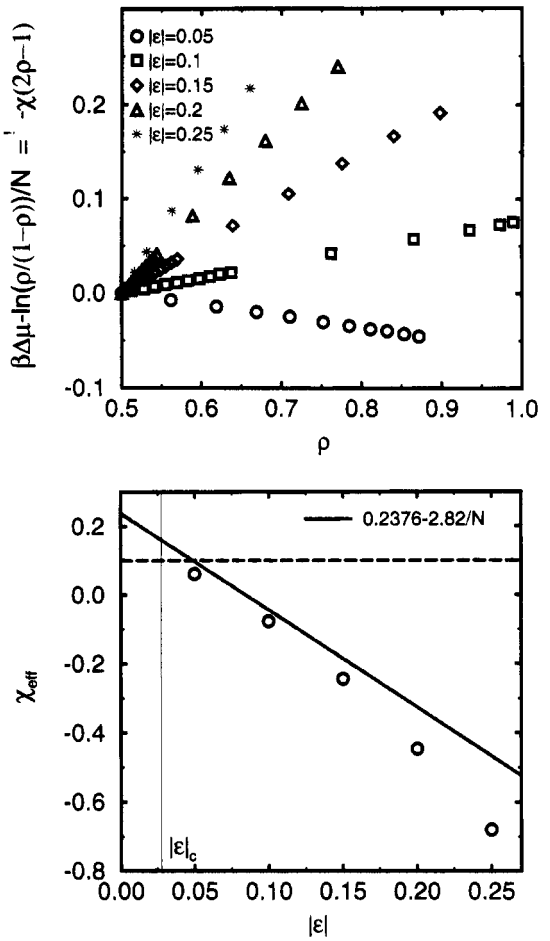

Figure 3. (a) Equation of state for chain length $N = 20$, system size $L = 40$, and different temperatures. The slope determines the effective χ parameter. (b) Temperature dependence of the χ parameter for the same system parameters.

First we examine mixtures of chain length $N = 20$. The mean field approximation suggests that the nonadditivity is strong enough and that the athermal system is not miscible. This is in accord with the simulation data. Therefore we introduce an attractive interaction between different species and find a LCSP. In the following we study the SG-EQS in the one-phase region, i.e. at low temperatures. Entropic packing induced corrections to the SG-EQS of state can be detected in the semi-grand-canonical ensemble easily, at least in principle. Therefore we resort to the definition (1.4) of the effective χ parameter and rewrite it in the form

$$\frac{\partial}{\partial\varrho}\left\{\beta\Delta\mu - \frac{1}{N}\ln\frac{\varrho}{1-\varrho}\right\} = -2\left(2z_c\epsilon - \frac{1}{2}\frac{\partial\Delta S}{\partial\varrho}\right) \equiv -2\chi_{\text{eff}} \tag{2.10}$$

i.e. the slope of the difference between the measured SG-EQS and the exact combinatorial contribution gives the effective χ. Since the system is symmetric with respect to a global interchange of the labels A and B, we restrict ourselves to an A-rich mixture. The simula-

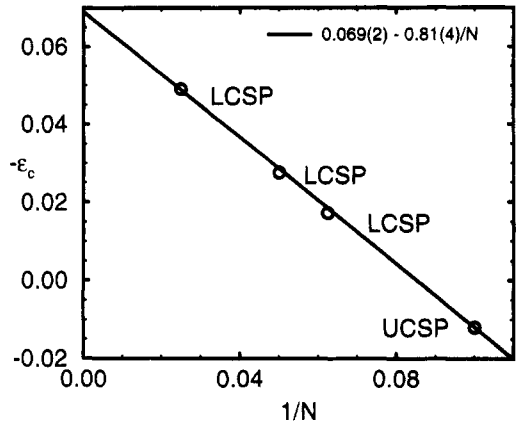

Figure 4. Chain length dependence of the critical temperature for mixtures of nonadditive monomers. The straight line is given by $\epsilon_c = 0.069(2) - 0.81(4)(1/N)$.

tion data, shown in Figure 3a, can be well approximated by a straight line. Therefore the χ parameter is roughly independent of composition, in accord with the mean field approximation. By linear regression we determine χ, whose temperature dependence is shown in part b. By a separate simulation at $\varrho = 1/2$, we also calculate the effective coordination numbers z_6 and z_c, which parametrize the local structure of the monomer fluid. At $|\epsilon| = 0.05$ we find $z_6 = 0.238(2)$ in an additive mixture and $z_c = 1.41(2)$ in a nonadditive mixture. The predictions of our mean field calculations are also shown in Figure 3b and agree rather well with the simulation data. In the vicinity of the critical point, strong fluctuations of the composition lead to deviations from the mean field approach. These fluctuations stabilize the mixture, such that the mean field theory underestimates the critical temperature. Whereas at lower temperatures the discrepancies can probably be traced back to a slight temperature dependence of the effective coordination numbers. Extrapolating the simulation data to the athermal limit, one can estimate the entropic contribution to the χ parameter to $\Delta\chi = 0.20(2)$.

Next we study the chain length behavior of the critical temperature. In accord with previous studies[16] we use multihistogram extrapolation[13,14] and the cumulant intersection method[11] to locate accurately the critical point along the coexistence curve. As anticipated, the athermal system is miscible for short chain lengths ($N = 10$) and we find an upper citical solution point (UCSP). For longer chains ($N = 16, 20, 40$) the system is immiscible in the athermal limit and, using an attractive interaction between different species, we observe a LCSP. The chain length dependence of the critical temperature is well described by an effective behavior of the form

$$-\epsilon_c = A - \frac{B}{N} \quad \text{with} \quad A = 0.069(2) \text{ and } B = 0.81(4) \tag{2.11}$$

This determines the critical chain length to $N_c = 12$. Using the measured effective coordination numbers, the mean field calculation gives $A = 0.084$, $B = 0.71$, and $N_c = 8.4$. The deviations from the mean field approximation are mainly due to composition fluctuations, which tend to stabilize the mixture. Note that we find 3D Ising critical behavior at T_c, in agreement with previous simulations[16] and experiments.[10] Further discrepancies arise, due to the factorization approximation in eq 2.6 and a chain length dependence of the effective coordination numbers[19] z_6 and z_c, caused by correlation hole effects.

3. Polymer Blends with Different Stiffnesses

The previous section illustrates the importance of local packing effects on the phase behavior. Within the semi-grand-canonical ensemble it is possible to reveal these entropic effects either via the SG-EQS or the critical temperature. In the second part, we want to employ the techniques explained above to investigate a second structural disparity. Differences in the chemical microstructure manifest themselves not only by steric packing effects but also via different spatial extensions of the chemical repeat units or by variable persistence lengths, i.e. chain stiffness disparities. It is known from simple liquids, that strong asymmetries in the monomer size may lead to an entropy-driven phase separation. This effect has been discussed also in the context of solvent-induced collapse in polymer solutions,[27] and the modeling of various monomer shapes in polymer blends has found widely spread application in the framework of the lattice cluster theory by Freed.[7]

Here, however, we consider a polymer blend, whose species differ in their chain stiffness. This common asymmetry is of great practical importance[1,3,28] and therefore has found some experimental[6] and theoretical interest.[8,9] Whereas the nonadditive monomer shapes or size disparities result in local packing effects, stiffness disparity is a truly polymeric feature, which length scale is between the local, monomeric size and the radius of gyration.[9] Some previous Monte–Carlo studies have focused on these nonlocal packing effects. Recent Monte-Carlo simulations and integral equation theories by Yethiraj et al.[29] investigated an athermal mixture of flexible and stiff chains in the vicinity of a hard wall. They found an entropy-driven surface segregation of the stiffer chains at meltlike densities, because the stiffer species packs more efficiently at the hard wall. Previous Monte-Carlo simulations by Gauger and Pakula[30] investigated a mixture of flexible and very stiff chains in the canonical ensemble and used the subblock method[31] to analyze their simulation data. Solely due to the stiffness and the excluded volume constraints, they found evidence for a separation into a pure phase of stiff chains and a phase of mixed composition. The present investigation focuses on rather small differences in the chain stiffness, such that both flexible and stiff chains can be described as Gaussian chains with different persistence lengths.

In order to mimic this polymeric feature within the framework of the bond fluctuation model, the B polymers are stiffened by imposing an intermolecular potential, which favors straight bond angle conformations. We use a particularly simple choice:[32]

$$E(\theta) = f \cos\theta \tag{3.12}$$

where θ denotes the complementary angle of two successive bonds. The large number of bond vectors permits 87 different bond angles. This property of the bond fluctuation model allows an implementation of chain stiffness, which is rather close to its analogue in continuous space. As in the previous section, we use a thermal square well potential, which is extended over the first 54 neighbor sites and which favors phase separation of the two species. In accord with previous studies,[16,19] we work at a filling fraction of $8\Phi = 0.5$, corresponding to a dense melt.[22] Monomers are represented by cubes, as in the original version. Within the Flory–Huggins mean field approximation the bond

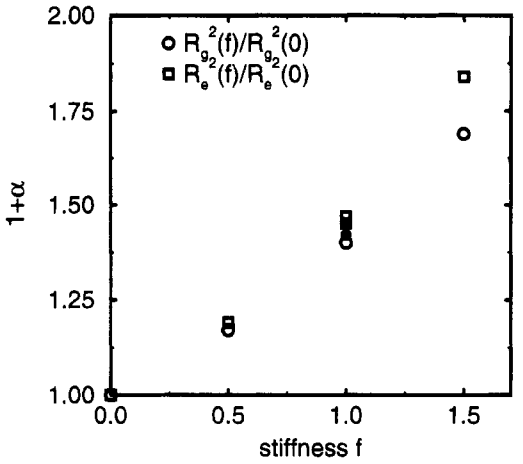

Figure 5. Configurational data of stiff and flexible chains at criticality. $\alpha \equiv [R^2(f)/R^2(0)] - 1$ describes the disparity between flexible and stiff chains.

Table 2. Configurational Data for Stiff and Flexible Chains at Criticality

N	f	$R_g^2(0)$	$R_e^2(0)$	$R_g^2(f)$	$R_e^2(f)$
16	0.5	22.5(4)	131(2)	26.5(4)	157(2)
	1.0	22.7(4)	132(2)	31.7(4)	193(2)
	1.5	22.7(4)	132(2)	38.3(4)	241(2)
32	1.0	48.5(8)	288(4)	68.9(8)	418(4)

stiffness results in the following additional term in the free energy density:

$$\frac{\beta\Delta f}{\Phi} = f\overline{\cos\theta}\frac{N-2}{N}(1-\varrho) \qquad (3.13)$$

where $\overline{\cos\theta}$ denotes the average bond angle. The chain length dependence results from the fact that a chain of N segments includes only $N-2$ bond angles. Thus there is no additional contribution to the χ parameter within this approximation. Only the coexistence exchange potential is shifted

$$\beta\Delta\mu_{\text{coex}} = -f\overline{\cos\theta}\frac{N-2}{N} \qquad (3.14)$$

to account for the reduction of chain conformations due to the stiffness. However, a possible composition dependence of the number of states of a single chain is not included.

The implementation of the semi-grand-canonical Monte-Carlo steps is conceptually straightforward. In addition to the thermal energy difference, one has to account for the bending energy in an attempted identity switch. In the simulations we employ the following ratios of Monte-Carlo moves: randon hopping:slithering snake:semi-grand-canonical = 1:3:1. The configurational data of the simulated systems are gathered in Table 2. Note that the spatial extension of the flexible chains is independent of the stiffness parameter f. Increasing the stiffness f, the B polymers prefer a stretched configuration of successive bonds. This increase can be monitored by the end-to-end distance or the radius of gyration, as presented in Figure 5. The discrepancies between the ratios of R_e^2 and R_g^2 for $N = 16$ and $f = 1.5$ indicate that there are already deviations from Gaussian chain statistics for such large stiffnesses and short chain lengths.

However, simulating large stiffness asymmetries and chain lengths becomes quite demanding in terms of CPU-time requirements. With growing disparity of the two species the acceptance rate of the semi-grand-canonical Monte-Carlo steps rapidly decreases, because each pair of successive bonds contributes to the bending energy. In the worst case studied ($N = 32, f = 1.0, L = 56$) the correlation time of composition fluctuations exceeds corresponding values of symmetrical mixtures ($f = 0$)[16] by 3 orders of magnitude. Therefore the simulation of very long and stiff chains in the semi-grand-canonical ensemble is hardly feasible.

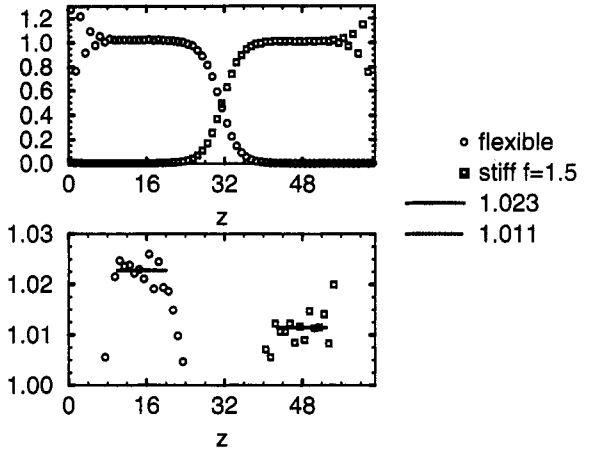

Figure 6. Interfacial profile of the normalized monomer density in a blend of stiff ($f = 1.5$) and flexible polymers well below criticality $T = 0.346T_c$. The simulation box $32 \times 32 \times 64$ has hard walls in the z direction. The enlargement shows that vacancies are enriched in the stiffer phase (right-hand side).

Even within this rather simple model, the thermodynamic behavior is somewhat more complicated compared to the mixtures with nonadditive monomers. There are several reasons for deviations from the simple mean field picture:

•Neglecting composition fluctuation, the mean field theory is not appropriate in the vicinity of the critical point.

•Due to the chain stiffness a folding back of the stiffer species is less probable. Therefore the number of contacts with *other* chains increases. This influences the effective thermal coordination number $z_c = (z_{AA} + z_{BB})/2 + z_{AB}$ and leads to an increase of the critical temperature. This effect has also been noted in the micellization of diblock copolymers with blocks of different stiffnesses.[33]

•The mean field treatment neglects the composition dependence of the single chain entropy. The packing effects[29] at hard walls suggest that similar effects may lead to an entropic term in the effective χ parameter.

•At equal monomer density the osmotic pressure π of stiff chains is slightly higher than for flexible chains. This has been investigated in a two-dimensional version of the bond fluctuation model.[34] If there is a phase coexistence of a B-rich and a B-poor phase in the simulation cell, the vacancies will distribute as to restore equal osmotic pressure in both phases. Therefore the monomer density of the B-rich phase is lowered and the density of the A-rich phase is increased. This rather small effect is illustrated in Figure 6, which presents the composition profiles between coexisting unmixed phases of a mixture well below the critical point in the canonical ensemble. One observes that the monomer density difference of the coexisting phases is about 1%.

Here we focus our interest on the entropic packing effects due to the stiffness disparity. As illustrated above, these influence the SG-EQS and the critical temperature.

3.1. Athermal Semi-Grand-Canonical Equation of State. In the following we try to isolate the entropic packing effect by investigating the athermal SG-EQS. Since there are no thermal interactions, one need not resort to the mean field treatment of the composition fluctuations and the effective coordination number z_c does not enter the description. Thus deviations from the Flory–Huggins theory are exclusively due to entropic packing effects.

Going beyond the Flory–Huggins treatment, there are two analytical predictions for an athermal mixture: Schweizer and co-workers[35] use an integral equation approach and predict a negative entropic contribution to the χ parameter of the form

$$\Delta\chi = -\frac{\eta^2\Gamma^6}{6}\alpha^2(1+\alpha(1-\varrho)) \qquad (3.15)$$

where η denotes the packing fraction of their threadlike polymer model and Γ denotes the ratio between the statistical segment length and the thread diameter. $\alpha = R_B^2/R_A^2 - 1$ characterizes the difference of the statistical segment length. Therefore, stiffness disparity enhances the miscibility.

One the other hand Liu and Fredrickson[9] calculate within a field theoretical approach an entropic correction of the form

$$\Delta\chi = C\frac{1}{24\pi^2}\frac{\alpha^2}{(1+\alpha\varrho)^2} \qquad (3.16)$$

where C is a positive constant of order unity. Therefore the difference in the chain stiffness results in a nonlocal, noncombinatorial excess entropy, which favors demixing of the unlike species. In both cases the correction is of the order α^2 and independent of chain length. Therefore the latter treatment anticipates a LCSP or the immiscibility of an athermal system in the long chain large stiffness limit. However, note that the absolute value of $\Delta\chi$ is of the order 10^{-3} for $\alpha = 0.5$. Thus the entropic contribution is about 2 orders of magnitude smaller than for mixtures with indented monomer shapes.

The simulation data for the athermal SG-EQS are presented in Figure 7. The N dependent shift of the curves for $f = 1.0$ is due to the chain length dependence in eq 3.14. One observes a small, but clear, negative slope of the $\beta\Delta\mu - \ln\varrho/(1-\varrho)$ vs ϱ curve. This indicates a positive entropic contribution to the effective χ parameter. Since the quality of the simulation data does not permit an analysis in terms of a composition dependent χ, we determine an average χ parameter by a linear fit to the simulation data.

$N = 16$ $f = 1.0$ $\Delta\chi = 0.0017(2) \approx 0.014\chi_c$ with $\chi_c = 2/N$

$N = 16$ $f = 1.5$ $\Delta\chi = 0.0031(3) \approx 0.024\chi_c$

$N = 32$ $f = 1.0$ $\Delta\chi = 0.0018(2) \approx 0.028\chi_c$

Within statistical accuracy, we find evidence for a positive, chain length independent entropic $\Delta\chi$. Therefore these simulation data are in qualitative agreement with the predictions of Liu and Fredrickson.[9] Since the effect is rather small compared to the mean field prediction of the critical χ parameter, simulations in the semi-grand-canonical ensemble are not able to proceed to chain lengths where one would expect a LCSP, i.e. $N \approx O(1000)$. In view of the athermal simulation data, one rather anticipates a shift of the critical temperature of the order of a few percent.

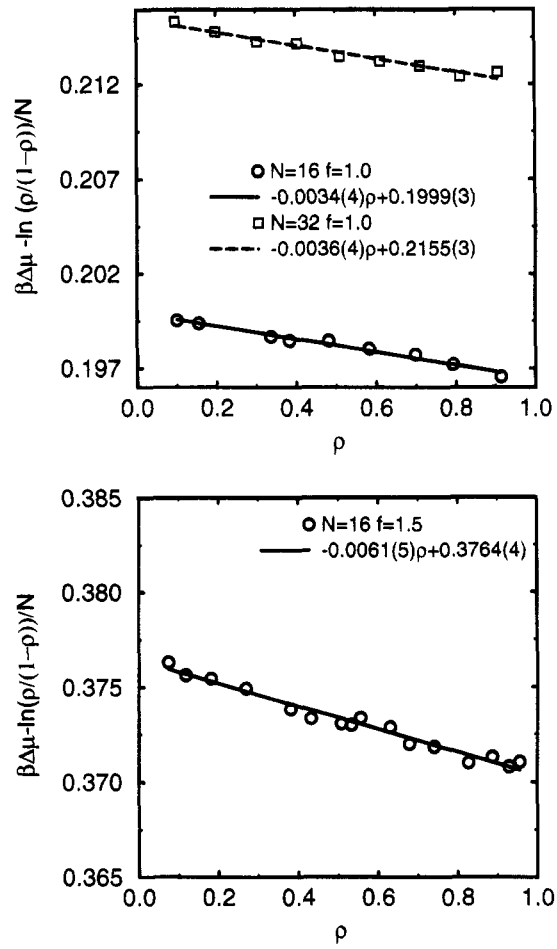

Figure 7. Deviations from the SG-EQS: (a) $N = 16$, $f = 1.0$, $L = 32$ and $N = 32$, $f = 1.0$, $L = 56$; (b) $N = 16$, $f = 1.5$, $L = 32$.

3.2. Critical Composition and Critical Density. Due to the lack of symmetry between A and B polymers, one has to locate the critical point in the two-dimensional parameter space of temperature and exchange potential. This can be achieved by locating the coexistence line and its analytical continuation above the critical point via the equal weight rule[36] and then using the cumulant intersection[11] along the coexistence line to determine the critical temperature. Histogram extrapolations[13,14] have been used to extrapolate the simulation data to nonsimulated values of temperature and exchange potential. The quality of the simulational data does not warrant a correction for field mixing effects. The more technical details of locating the critical point in grand-canonical simulations of asymmetric systems have been discussed in detail in refs 12 and 37.

For thermal blends, there exists a P-RISM calculation by Schweizer[8] relying on a new molecular closure. According to these calculations, there is no change in the critical temperature for the interaction potentials used in this study and the critical density is given by

$$\varrho_c = \frac{1+\alpha}{2+\alpha} \qquad (3.17)$$

The simulational results for the critical density are presented in Figure 8. The critical density is larger then $^1/_2$, but the shift is much smaller than predicted by the P-RISM theory. For $\alpha = 0.75$ the equation above predicts $\varrho_c \approx 0.64$, which clearly disagrees with the

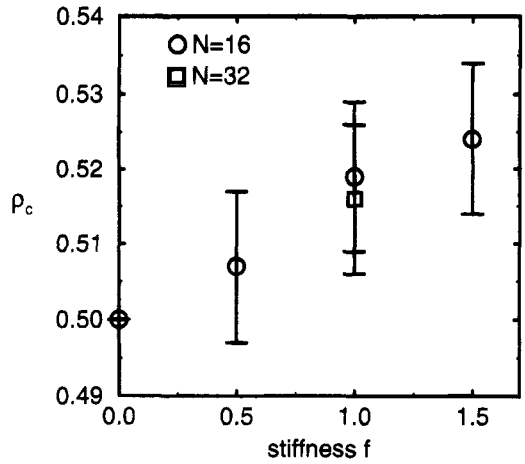

Figure 8. Dependence of the critical composition on the stiffness parameter f.

Monte-Carlo simulation. The approach by Liu and Fredrickson however predicts a critical density even smaller than $^1/_2$. At present we do not have any explanation of this effect; one might speculate that it is related to the osmotic pressure or nonuniversal local packing effects of the bond fluctuation model.

As shown in Figure 9a, the critical temperature is increased compared to symmetrical mixtures. There are two effects contributing to this increase: the positive entropic contribution to χ and the increase of the thermal coordination number. To separate these mechanisms, we have determined the coordination numbers z_c by a separate simulation at composition $\varrho = 0.5$. Within the mean field approximation the critical temperature is given by

$$\frac{2}{N} = 2z_c\epsilon_c + \Delta\chi \quad \Rightarrow$$

$$T_c = \frac{1}{\epsilon_c} = \frac{z_c N}{1 - \Delta\chi N/2} \approx z_c N\left(1 + \Delta\chi\frac{N}{2}\right) \quad (3.18)$$

Thus, within the mean field treatment, the ratio of T_c/z_c mirrors the increase due to the positive entropic contribution $\Delta\chi$. This behavior is illustrated in Figure 9b. Note that the effect for the chain length $N = 32$ is roughly twice as large as the shift for chain length $N = 16$. This is also an indication for the chain length independence of $\Delta\chi$. However, it should be remarked, that the mean field approach overestimates the critical temperature by about 25%, due to the inappropriate treatment of composition fluctuations. Thus the simple addition of the enthalpic and entropic contribution to the critical value of the χ parameter is not quantitatively correct for these short chain lengths. Nevertheless the magnitude is in agreement with the conclusion from the athermal SG-EQS. Thus, both the deviation from the SG-EQS and the increase of the critical temperature support evidence for a chain length independent, positive contribution to the effective χ parameter due to the chain stiffness disparity.

4. Summary and Outlook

In the present paper, we illustrate the effects of structural disparities on the thermodynamic behavior of polymer mixtures by Monte-Carlo simulations of the bond fluctuation model in the semi-grand-canonical ensemble. In principle, this ensemble is particularly advantageous, because the relaxation times of composition fluctuations are smaller than in the canonical ensemble and the SG-EQS is directly accessible. For

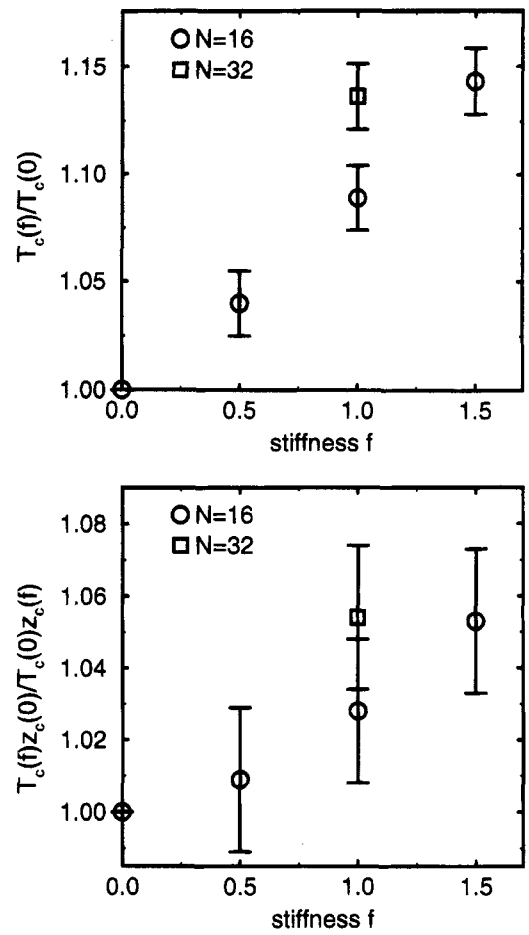

Figure 9. Dependence of the critical temperature (a) and the ratio between critical temperature and effective coordination number z_c (b) on the stiffness f.

Table 3. Critical Point Location of Blends with Different Stiffnesses[a]

N	f	ϵ_c	$N\beta\Delta\mu$	ϱ_c	z_c	system size
16	0	0.02766(15)	0	0.5	2.758(20)	24,32,40,48
	0.5	0.0266(3)	1.17	0.507(10)	2.841(20)	24,32,48
	1.0	0.0254(3)	3.20	0.519(10)	2.923(20)	24,32,48
	1.5	0.0242(3)	6.01	0.524(10)	2.993(20)	24,32,48
32	0	0.01422(6)	0	0.5	2.557(20)	24,32,40,56
	1.0	0.0127(1)	6.865	0.516(10)	2.755(20)	32,48,56

[a] Data of symmetrical mixtures are given by simulations of H. P. Deutsch.[16]

both model systems, mixtures with indented monomers and blends of polymers with different stiffnesses, our simulational results are compatible with a positive, chain length independent entropic contribution to the effective χ parameter. This contribution is detectable via corrections to the SG-EQS or a shift in the critical temperature. For the mixtures with indented monomers, the additional local packing contribution is rather large and leads to immiscibility of an athermal blend for $N > N_c$. Thus for $N > N_c$ and attractive thermal interactions between unlike polymers, one observes a thermally driven LCSP. In accordance with a mean field approximation, the lower critical solution temperature approaches a finite constant value from above.

However, the nonlocal influence of stiffness disparity is comparably smaller and leads only to an increase of the critical temperature in a mixture with repulsive thermal interactions of a few percent. The simulation data are in qualitative agreement with recent calculations of Liu, Fredrickson, and co-workers[9] and are also compatible with a phase separation for long chain

lengths and much larger stiffness disparity found by Gauger and Pakula.[30]

According to ref 9, these nonlocal packing effects manifest themselves also in mixtures of linear and star polymers. Using techniques similar to those in ref 18, it is possible to reveal entropic effects also in these systems. Possible future work might consider off-lattice models[38] of structurally asymmetric polymer blends. The semi-grand-canonical scheme in conjunction with constant pressure simulations may yield valuable information on the thermodynamics of mixtures. In the case of indented, nonadditive monomers, one anticipates a pronounced volume change upon mixing. Therefore the density dependence of the thermal interactions and the local packing structure may induce a composition dependence of the effective χ parameter. The constant volume simulations presented in Figure 6 also indicate the relevance of these effects for stiffness disparities. Furthermore the effect of different monomer volumes may be modelled in off-lattice models in a more natural way than in lattice models.

Acknowledgment. Its a great pleasure to thank K. Binder for introducing me to this topic and stimulating discussions. The author has also benefitted from helpful discussions with N. B. Wilding and W. Paul. Partial support from the Deutsche Forschungsgemeinschaft (DFG) under grant number Bi314/3-2 is also acknowledged.

References and Notes

(1) *Polymer Compatibility and Incompatibility, Principles and Practices*; Solc, K., Ed.; Haarwood Academic Publisher: Chur, 1980. *Polymer Blends and Composites in Multiphase Systems*; Han, C. D., Ed.; Advances in Chemistry Series 206; American Chemical Society: Washington, DC. *Material Science and Technology, a Comprehensive Treatment*; Cahn, R. W., Haasen, P., Kramer, E. J., Eds.; VCH: New York, 1993; Vol. 12.
(2) Honeycutt, J. D. *Macromolecules* **1994**, *27*, 5377.
(3) Lee, S.; Oertli, A. G.; Gannon, M. A.; Liu, A. J.; Pearson, D. S.; Schmidt, H. W.; Fredrickson, G. H. *Macromolecules* **1994**, *27*, 3955.
(4) Flory, P. J. *J. Chem. Phys.* **1941**, *9*, 660. Huggins, H. L. *J. Chem. Phys.* **1941**, *9*, 440.
(5) Bates, F. S.; Muthukumar, M.; Wignall, G. D.; Fetters, L. J. *J. Chem. Phys.* **1988**, *89*, 525.
(6) Bates, F. S.; Schultz, M. F.; Rosedale, J. H.; Almdal, K. *Macromolecules* **1992**, *25*, 5547.
(7) Dudowitz, J.; Freed, K. F.; Lifschitz, M. *Macromolecules* **1994**, *27*, 5387. Bawendi, M. G.; Freed, K. F. *J. Chem. Phys.* **1988**, *88*, 2741. Pesci, A. I.; Freed, K. F. *J. Chem. Phys.* **1989**, *90*, 2017. Dudowicz, J.; Freed, K. F.; Madden, W. G. *Macromolecules* **1990**, *23*, 4803. Madden, W. G.; Pesci, A. I.; Freed, K. F. *Macromolecules* **1990**, *23*, 1181.
(8) Scheweizer, K. S. *Macromolecules* **1993**, *26*, 6033, 6050.
(9) Liu, A. J.; Fredrickson, G. H. *Macromolecules* **1992**, *25*, 5551. Fredrickson, G. H.; Liu, A. J.; Bates, F. S. *Macromolecules* **1994**, *27*, 2503. Bates, F. S.; Fredrickson, G. H. *Macromolecules* **1994**, *27*, 1065.
(10) Schwahn, D.; Janssen, S.; Willner, L.; Schmackers, T.; Springer, T.; Mortensen, K.; Takeno, H.; Hasegawa, H.; Jinnai, H.; Hashimoto, T.; Imai, M. Preprint submitted to *Physica B*. Schwahn, D.; Takeno, H.; Willner, L.; Hasegawa, H.; Jinnai, H.; Hashimoto, T.; Imai, M. Preprint submitted to *Phys. Rev. Lett.* See also: Schwahn, D.; Mortensen, K.; Springer, T.; Yee-Madeira, H.; Thomas, R. *J. Chem. Phys.* **1987**, *87*, 6078.
(11) Binder, K.; Nauenberg, M.; Privman, V.; Young, A. P. *Phys. Rev. B* **1985**, *31*, 1498. Privman, V.; Fisher, M. E. *J. Stat. Phys.* **1985**, *33*, 385. Binder, K. *Z. Phys. B* **1985**, *13*. Barber, M. W. In *Phase Transitions and Critical Phenomena*; Domb, C., Green, C., Eds.; Academic Press: New York, 1983; Vol. 8. Privman, V. In *Finite Size Scaling and Numerical Simulation of Statistical Systems*; Privman, V., Ed.; World Scientific: Singapure, 1990. Binder, K. *Z. Phys. B* **1981**, *43*, 119. *Phys. Rev. Lett.* **1981**, *47*, 693. Binder, K. In *Computational Methods in Field Theory*; Gausterer, A., Lang, C. B., Eds.; Springer: Berlin 1992; p 59 K. Binder,K. Landau, D. P. *Phys. Rev. B* **1984**, *30*, 1477. Binder, K. *Z. Phys. B* **1981**, *43*, 119.
(12) Bruce, A. D.; Wilding, N. B. *Phys. Rev. Lett.* **1992**, *68*, 193. Wilding, N. B.; Bruce, A. D. *J. Phys. Condens. Matter* **1992**, *4*, 3087. Wilding, N. B. *Z. Phys. B* **1993**, *93*, 119.
(13) Ferrenberg, A. M.; Swendsen, R. H. *Phys. Rev. Lett.* **1988**, *61*, 2635; **1989**, *63*, 1195. Bennett, A. *J. Comput. Phys.* **1979**, *22*, 245.
(14) Deutsch, H. P. *J. Stat. Phys.* **1992**, *67*, 1039.
(15) Sariban, A.; Binder, K. *J. Chem. Phys.* **1097**, *86*, 5859. Sariban, A.; Binder, K. *Colloid Polym. Sci.* **1988**, *266*, 389. Sariban, A.; Binder, K. *Macromolecules* **1988**, *21*, 711. Binder, K. *Colloid Polym. Sci.* **1988**, *266*, 871. Sariban, A.; Binder, K. *Colloid Polym. Sci.* **1989**, *267*, 469. Sariban, A.; Binder, K. *Macromolecules* **1991**, *24*, 587. Binder, K.; Deutsch, H. P.; Sariban, A. *J. Non-Cryst. Solids* **1991**, *131*, 635.
(16) Deutsch, H. P.; Binder, K. *Europhys. Lett.* **1992**, *17*, 697. Binder, K.; Deutsch, H. P. *Europhys. Lett.* **1992**, *18*, 667. Deutsch, H. P.; Binder, K. *Macromolecules* **1992**, *25*, 6214. Deutsch, H. P.; Binder, K. *J. Phys. II* **1993**, *3*, 1049.
(17) Deutsch, H. P. *J. Chem. Phys.* **1993**, *99*, 4825. Deutsch, H. P.; Binder, K. *Die Makromol. Chem. Macromol. Symp.* **1993**, *65*, 59. Deutsch, H. P.; Binder, K. *Polym. Prepr.* **1992**, *33*, 698.
(18) Müller, M.; Binder, K. *Comput. Phys. Commun.* **1994**, *84*, 173.
(19) Müller, M.; Binder, K. *Macromolecules* **1995**, *28*, 1825.
(20) Carmesin, I.; Kremer, K. *Macromolecules* **1988**, *21*, 2819. Wittmann, H. P.; Kremer, K. *Comput. Phys. Commun.* **1990**, *61*, 309. Deutsch, H. P.; Binder, K. *J. Chem. Phys.* **1991**, *94*, 2294.
(21) Yethiraj, A.; Dickman, R. *J. Chem. Phys.* **1988**, *97*, 1704.
(22) Paul, W.; Binder, K.; Heermann, D. W.; Kremer, K. *J. Phys. II* **1991**, *1*, 37. *J. Chem. Phys.* **1991**, *95*, 7726.
(23) Paul, W.; Pistoor, N. *Macromolecules* **1994**, *27*, 1249. Paul, W.; Binder, K.; Batoulis, J.; Pittel, B.; Sommer, K. H. *Polym. Prepr. (Am. Chem. Soc., Div. Polym. Chem.)* **1992**, *33*, 535. *Makromol. Chem., Macromol. Symp.* **1992**, *65*, 1.
(24) Frenkel, D.; Louis, A. A. *Phys. Rev. Lett.* **1992**, *68*, 3363. Schneider, F. Diploma thesis, Mainz, 1992. Ihm, M. O. Dipolma thesis, Mainz, 1993. Ihm, M. O.; Schneider, F.; Nielabla, P. Preprint Mainz, 1994.
(25) However, if the mixture was at a fixed pressure rather than at a fixed volume, even in the absence of thermal interactions, the density/pressure dependence of N_c might induce an athermal phase transition as a function of pressure.
(26) Paul, W.; Binder, K.; Kremer, K.; Heermann, D. W. *Macromolecules* **1991**, *24*, 6332.
(27) Dijkstra, M.; Frenkel, D.; Hansen, J-P. *J. Chem. Phys.* **1994**, *101*, 3179.
(28) Ballauff, M. *Ber. Bunsen Ges. Phys. Chem.* **1986**, *90*, 1053. See e.g.: Flory, P. J. *Macromolecules* **1978**, *11*, 1138.
(29) Yethiraj, A.; Kumar, S. K.; Hariharan, A.; Schweizer, K. S. *J. Chem. Phys.* **1994**, *100*, 4691.
(30) Gauger, A.; Pakula, T. *J. Chem. Phys.* **1993**, *98*, 3548. Gauger, A. Thesis, Mainz, 1993 (unpublished).
(31) Rovere, M.; Heermann, D. W.; Binder, K. *Europhys. Lett.* **1988**, *6*, 585; *J. Phys.: Condens. Matter* **1990**, *2*, 7009. Rovere, M.; Nielaba, P.; Binder, K. *Z. Phys. B* **1993**, *90*, 215.
(32) Wittmer, J.; Paul, W. Binder, K. *Macromolecules* **1992**, *25*, 7211. Wittmer, J.; Paul, W.; Binder, K. *J. Phys. II* **1994**, *4*, 873. Wittmer, J. Diploma thesis, Mainz, 1991 (unpublished).
(33) Adriani, P.; Wang, Y.; Mattice, W. L. *J. Chem. Phys.* **1994**, *100*, 7719.
(34) Dickman, R. *Comput. Polym. Sci.* **1991**, *1*, 206.
(35) Curro, J. G.; Schweizer, K. S. *Macromolecules* **1990**, *23*, 1402. Honell, K. G.; Curro, J. G.; Schweizer, K. S. *Macromolecules* **1990**, *23*, 3496.
(36) Borgs, C.; Kotecky, R. *J. Stat. Phys.* **1990**, *61*, 79. Borgs, C.; Kotecky, R. *Phys. Rev. Lett.* **1992**, *68*, 1734. Borgs, C.; Kotecky, R.; Miracle-Sole, S. *J. Stat. Phys.* **1990**, *62*, 519. Borgs, C.; Kappler, S. *Phys. Lett.* **1992**, *A171*, 37.
(37) Müller, M.; Wilding, N. B. *Phys. Rev. E* **1995**, *51*, 2079. Wilding, N. B.; Müller, M. *J. Chem. Phys.* **1995**, *102*, 2562.
(38) Kumar, S. K. *Macromolecules* **1994**, *27*, 260.

MA946355I